High Frequency LLC Resonant Converter with Magnetic Shunt Integrated Planar Transformer

Li, Mingxiao; Ouyang, Ziwei; Andersen, Michael A. E.

Published in:
I E E E Transactions on Power Electronics

Link to article, DOI:
10.1109/TPEL.2018.2842029

Publication date:
2018

Document Version
Peer reviewed version

This article has been accepted for publication in a future issue of this journal, but has not been fully edited. Content may change prior to final publication. Citation information: DOI 10.1109/TPEL.2018.2842029, IEEE Transactions on Power Electronics

High Frequency LLC Resonant Converter with Magnetic Shunt Integrated Planar Transformer

Mingxiao Li, *Student Member, IEEE*, Ziwei Ouyang, *Senior Member, IEEE*, Michael A. E. Andersen , *Member, IEEE*
Department of Electrical Engineering, Technical University of Denmark, Kgs. Lyngby, Denmark
Corresponding author: Ziwei Ouyang, email: zo@elektro.dtu.dk

***Abstract*—Achieving high efficiency and high power density is emerging as a goal in many power electronics applications. LLC resonant converter has been proved as an excellent candidate to achieve this goal. To achieve smaller size of passive components, the resonant inductor in the LLC converter is usually integrated into the transformer by utilizing its leakage inductance. However, the leakage inductance of transformer is usually insufficient and thus the LLC converter has to be operated in a limited frequency range (this limits the input voltage range accordingly), otherwise the power efficiency will drop dramatically. Therefore, a larger resonant inductance in the LLC converter is expected to operate in a wider input voltage range. This paper proposes a new method to create a larger resonant inductance by using a magnetic shunt integrated into planar windings. The accurate leakage inductance modelling, calculation and optimal design guideline for LLC planar transformer, including optimal magnetic shunt selection and winding layout, are presented. A 280-380V input and output 48V-100W half bridge LLC resonant converter with 1MHz resonant frequency is built to verify the design methodology. A comparison is made between two converters with the same parameters, one using magnetic shunt integrated transformer and the others using traditional planar transformer and external inductor. Experimental result shows the proposed converter with magnetic shunt is capable to achieve comparable high efficiency and regulation capability with the other under a wide input voltage, which verify the optimal design methodology. Above all, this magnetics integration methodology reduces the whole converter's volume and thus increases the power density.**

***Index Terms*—magnetic shunt, LLC resonant converter, planar transformer, high frequency, wide input voltage.**

I. INTRODUCTION

There has been a long desire for converter miniaturization to increase its power density and efficiency. Resonant converters are capable to achieve soft switching and operate at high frequency [1]-[3]. LLC resonant converter has been proved as an excellent candidate to satisfy these requirements by increasing its switching frequency and integrating its magnetic components. It has become a popular converter and been used in many applications [4]-[11].

It is well understood that there is a strong trade-off between the input-voltage and/or output-voltage range and the power conversion efficiency. This trade-off is more severe in resonant converters than in pulse-width-modulated (PWM) converters. LLC resonant converters regulate the voltage by changing the switching frequency. They suffer from progressively increased losses when the input voltage is widened so that the typical LLC converters are not able to maintain high efficiency across the entire range when input voltage is wide. Some publications focus on decreasing magnetizing inductance to obtain high voltage gain [12]-[14]. The literature [12] proposes a transformer structure with auxiliary small inductance connected in parallel with the magnetizing inductance and controlled by a switch. The switch turns on to decrease the equivalent magnetizing inductance so as to obtain the high voltage gain. In literature [13], a capacitor is connected in series with the magnetizing inductance. When the switching frequency drops, the equivalent magnetizing inductance decreases so that the peak voltage gain increases. The other approach with auxiliary LC resonant circuit is proposed in [14] and is utilized to compensate the voltage gain. Although these methods [12]-[14] show high performance by optimal design methodology, they all require additional passive devices or power stage and none of them tests their methodology in high frequency-MHz operation.

An alternative to obtain high voltage gain with narrowed operating frequency range can be achieved by designing a large resonant inductor to create a low inductance ratio of magnetizing inductance to resonant inductance. If discrete magnetic components are used for LLC resonant converter, the large inductor may require extra winding loss and core loss, as well as large size of the component [15]-[20]. Therefore the resonant inductor is usually integrated into the transformer by utilizing its leakage inductance to increase its power density and efficiency especially when LLC converter operates at high frequency [25]-[28]. Interleaved structure is often implemented to reduce AC resistance [21]-[24], but causing a small leakage inductance and a large inductance ratio and leading to reduced regulation capability. When the primary and secondary windings are not interleaved [25]-[26], the leakage inductance can be utilized to replace the resonant inductance. However, the leakage inductance is still insufficient and hard to deal with wide input voltage.

This paper is to create a large leakage inductance of planar transformer by inserting a magnetic shunt into the transformer. The relation between the leakage inductance and the characteristic of magnetic shunt is investigated in [30].

Partial work is from the papers published in IECON 2017 [30] and APEC 2018 [31].
Authors are all from Technical University of Denmark, Kgs. Lyngby, 2800 Denmark.

This article has been accepted for publication in a future issue of this journal, but has not been fully edited. Content may change prior to final publication. Citation information: DOI 10.1109/TPEL.2018.2842029, IEEE Transactions on Power Electronics

Separating the primary and secondary windings away from the magnetic shunt further improve the leakage inductance while the winding loss due to the fringing effect is also minimized. The proposed integrated transformer structure and design methodology maintain the optimal magnetizing inductance while increasing leakage inductance to obtain a narrowed switching frequency band to deal with wide input voltage range. Thus high power efficiency is ensured with an optimal magnetizing inductance and high regulation capability is achieved with a small inductance ratio.

This paper is organized as follows. Section II analyzes the resonant tank design for the LLC resonant converter with high regulation capability. Section III elaborates the calculation and analysis of the leakage and magnetizing inductance for the proposed transformer structure. Section IV gives detailed design considerations for the proposed transformer structure and high performance LLC converter. In section V, a converter prototype with 1MHz 100W is built to demonstrate the proposed transformer structure, and a comparison with the discrete LLC converter using the external inductor connected in series with traditional transformer is made to verify the advantage of high power density and high efficiency. Section VI concludes this paper.

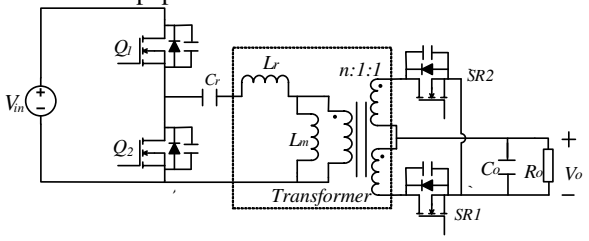

Fig.1. Topology of half bridge LLC resonant converter[31]

II. LLC Resonant Tank Design

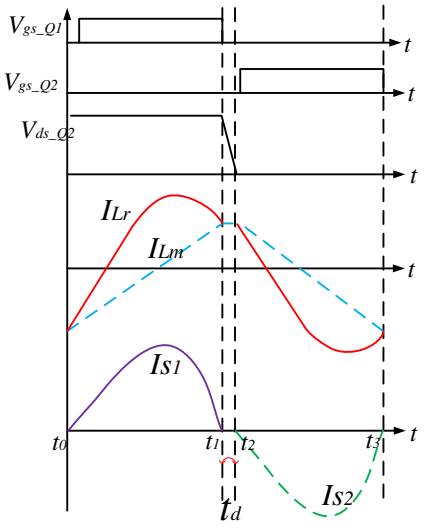

Fig.2. LLC resonant converter waveforms at resonant frequency

Fig.1 shows the half bridge LLC converter topology. Waveforms at the resonance are illustrated in Fig.2. When Q1 turns on, the magnetizing inductance L_m is charged and the magnetizing current I_{Lm} linearly grows until Q1 turns off at t_1. The drain-to-source voltage of Q2 V_{ds_Q2} drops to zero from t_1 to t_2 to achieve ZVS turn-on, where the output capacitance of Q2 is fully discharged by the magnetizing current.

It is known that LLC resonant converter can achieve maximum efficiency at resonant frequency, because there is no circulating energy loss. However, to achieve high voltage gain, the switching frequency of LLC resonant converter usually swings below the resonant frequency. The converter with higher regulation capability can operate at narrowed switching frequency band, which gives lower circulating energy loss and high efficiency compared to the converter with a lower regulation capability. The regulation capability is mainly affected by the inductance ratio of the magnetizing inductance L_m to the resonant inductance L_r. This relation is illustrated in Fig.3. The following description in this section gives a method to select the reasonable inductance ratio based on a specified voltage gain.

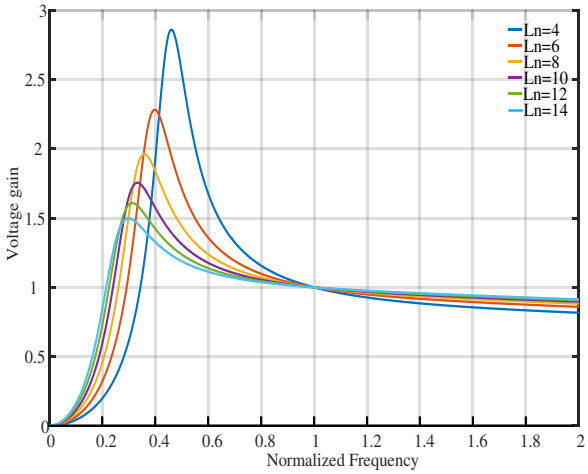

Fig.3. L_n impacts on LLC converter voltage gain

Resonant frequency f_r formed by resonant inductor L_r and resonant capacitor C_r, quality factor Q and inductance ratio L_n are important parameters to be considered:

$$f_r = \frac{1}{2\pi\sqrt{L_r C_r}} \tag{1}$$

$$Q = \frac{\sqrt{L_r/C_r}}{R_e}, \quad where \quad R_e = \frac{8n^2 R}{\pi^2} \tag{2}$$

$$L_n = \frac{L_m}{L_r} \tag{3}$$

Assume optimal magnetizing inductance is obtained. The real quality factor varies with L_n is expressed in (4) by combining (1), (2) and (3).

$$Q_{real} = \frac{L_m}{L_n}\frac{2\pi f_r}{R_e} \tag{4}$$

The maximum quality factor Q_{max} that allows the required maximum voltage gain at the boundary between capacitive and inductive mode is indicated in [27]

$$Q_{\max} = \frac{1}{L_n M_{\max}}\sqrt{L_n + \frac{M_{\max}^2}{M_{\max}^2 - 1}} \tag{5}$$

This article has been accepted for publication in a future issue of this journal, but has not been fully edited. Content may change prior to final publication. Citation information: DOI 10.1109/TPEL.2018.2842029, IEEE Transactions on Power Electronics

For a given specification, the maximum voltage gain M_{max} is specified. Thus the maximum quality factor is only varied with the inductance ratio L_n. This is also seen in minimum operating frequency that allows the converter to achieve the maximum voltage gain, which is expressed by

$$f_{n\_\min} = \sqrt{\frac{1}{1+L_n\left(1-1/M_{\max}{}^2\right)}} \tag{6}$$

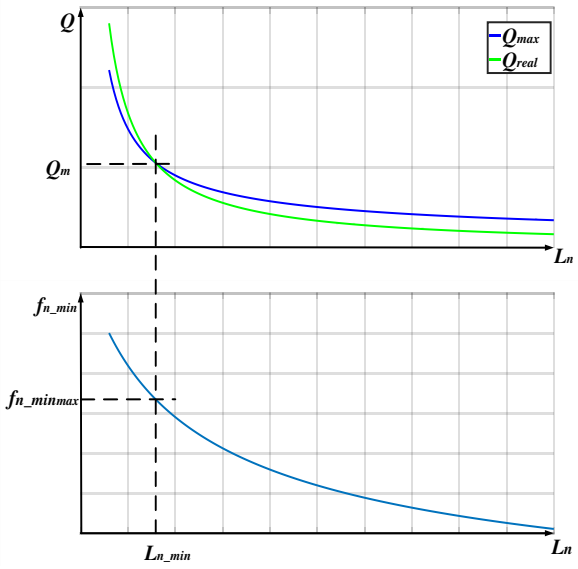

Fig.4. Quality factor and minimum operating frequency as a function of inductance ratio[31]

Based on (4), (5) and (6), the maximum quality factor Q_{max}, the real quality factor Q_{real}, and the minimum operating frequency f_{n_min} as a function of the inductance ratio are plotted in Fig.4. The real quality factor must be always below the maximum quality factor. The selected inductance ratio should be always larger than L_{n_min}, in order to allow the Q_{real} to be smaller than the Q_m. Nevertheless, a larger L_n allows a wider switching frequency range for a given voltage gain, and thus the regulation capability of the converter becomes weaker. Taken together, the inductance ratio L_n should be designed carefully to achieve ZVS in a full load range and obtain a narrowed switching frequency range. A small inductance ratio is expected to achieve high regulation capability. This implies a large resonant inductance L_r is needed in the assumption of unchanged magnetizing inductance L_m. The large resonant inductance may require extra windings and magnetic cores. This may cause additional power loss and increase the converter's volume. This paper integrates the large resonant inductance into the transformer by using magnetic shunt. The detailed analysis is shown as follows.

III. Proposed Integrated Transformer Structure

The proposed transformer structure is shown in Fig.5. Magnetic shunt is inserted in between the two magnetic cores. Both primary and secondary windings are located away from the magnetic shunt with controllable distances x_p and x_s respectively. The air gaps l_{ap} and l_{as} are inserted in between the magnetic cores and the magnetic shunt to get a desired magnetizing inductance, while the gaps have negligible effect on leakage inductance. The magnetizing inductance and leakage inductance in this configuration are modelled and analyzed in the following description.

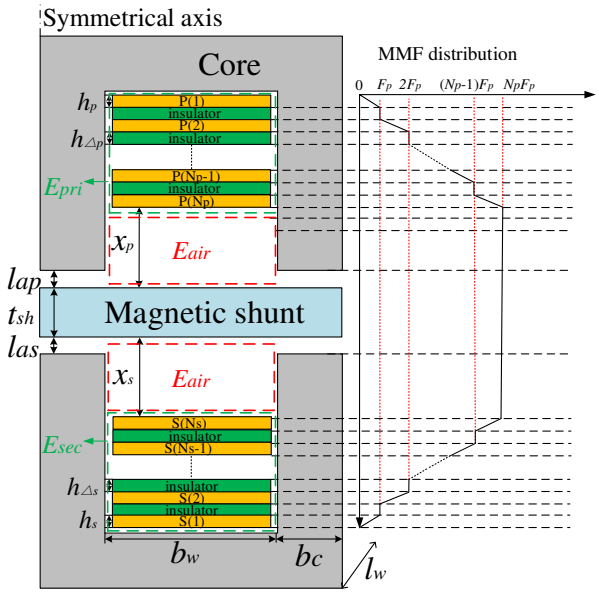

Fig.5. transformer with air gaps and both primary and secondary windings away from the shunt

The leakage energy contains the energy stored within the primary and secondary windings, the window air between windings, and the magnetic shunt. The leakage inductance is obtained by

$$E = \frac{1}{2}\int_V B \times H dV = \frac{1}{2}\cdot L_k \cdot I_p{}^2 \tag{7}$$

where V is the total effective volume; B is the flux density; H is the magnetic field, L_k is the leakage inductance and I_p is the primary current. The leakage energy stored in different elements can be calculated individually with the following sections:

A. Leakage energy stored in window area E_{air}

The magnetomotive force (MMF) in each layer of the primary windings is $F_p=k_p \cdot I_p$, where k_p is the number of turns on each layer of primary windings. N_p is the number of layers for primary winding. The MMF within the window area E_{air} can be assumed to be $N_p \cdot F_p$. The magnetic field intensity within the air area E_{air} is

$$H_{air} = \frac{N_p F_p}{b_w} \tag{8}$$

where b_w is the window width. Then the energy stored in the air is

$$E_{air} = \frac{1}{2}\mu_0 \cdot l_w \cdot b_w \int H^2 dx \tag{9}$$

where l_w is the winding mean turn length (MTL). Applying (8) into (9), the energy stored in the air is

$$E_{air} = 2\cdot\frac{1}{2}\mu_0 \cdot l_w \frac{N_p{}^2 k_p{}^2 I_p{}^2}{b_w}(x_p + x_s) \tag{10}$$

where x_p and x_s are the distances from the primary and secondary windings to the shunt, respectively.

This article has been accepted for publication in a future issue of this journal, but has not been fully edited. Content may change prior to final publication. Citation information: DOI 10.1109/TPEL.2018.2842029, IEEE Transactions on Power Electronics

B. *Leakage energy stored in primary and secondary windings*

Similarly, the leakage energy stored in the primary and secondary windings including the energy stored in the dielectric layers can be calculated from the MMF distribution [29]-[33], which are

$$E_{pri}=\frac{1}{6}\mu_0\frac{l_w}{b_w}k_p{}^2\left[h_{\Delta p}\left(2N_p{}^3-3N_p{}^2+N_p\right)+2h_pN_p{}^3\right]I_p{}^2 \quad (11)$$

$$E_{\sec}=\frac{1}{6}\mu_0\frac{l_w}{b_w}k_s{}^2\left[h_{\Delta s}\left(2N_s{}^3-3N_s{}^2+N_s\right)+2h_sN_s{}^3\right]I_s{}^2 \quad (12)$$

where $h_{\Delta p}$ and $h_{\Delta s}$ are the thickness of the dielectric layer of the primary winding and the secondary winding respectively.

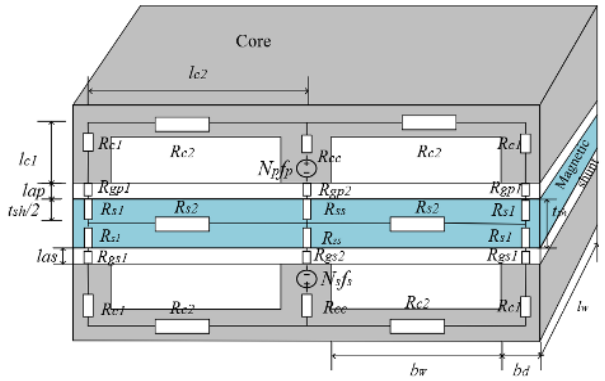

Fig.6. 3D structure of the proposed transformer

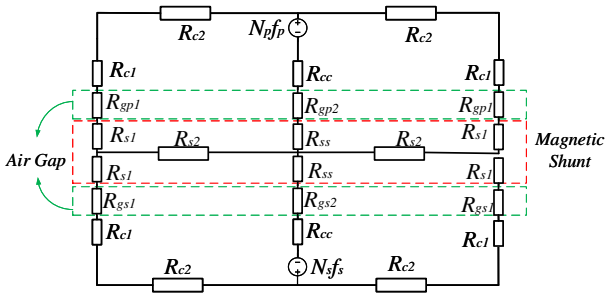

Fig.7. Magnetic reluctance model of the shunt-inserted planar transformer with air gaps [31]

C. *Leakage inductance created by magnetic shunt*

The reluctance model is utilized to obtain the leakage inductance created by the magnetic shunt. Fig.6 shows the structure of the planar transformer, and the magnetic reluctance model is illustrated in Fig.7. The air gaps are created in each leg in between the magnetic cores and the magnetic shunt. The reluctances of the sectional magnetic cores R_{c1}, R_{c2}, R_{cc}, the reluctances of the sectional magnetic shunts R_{s1}, R_{s2}, R_{ss} and the reluctances of the air gaps R_{gp1}, R_{gp2}, R_{gs1}, R_{gs2} indicated in Fig.6 are specified by

$$R_{c1}=\frac{l_{c1}}{\mu_0\cdot\mu_r\cdot b_d\cdot l_w},\quad R_{c2}=\frac{l_{c2}}{\mu_0\cdot\mu_r\cdot b_d\cdot l_w}$$

$$R_{cc}=\frac{l_{c1}}{\mu_0\cdot\mu_r\cdot A_c},\quad R_{s1}=\frac{t_{sh}}{2\mu_0\cdot\mu_s\cdot b_d\cdot l_w}$$

$$R_{s2}=\frac{b_w}{\mu_0\cdot\mu_s\cdot t_{sh}\cdot l_w},\quad R_{ss}=\frac{t_{sh}}{2\mu_0\cdot\mu_s\cdot A_c}$$

$$R_{gp1}=\frac{l_{ap}}{\mu_0\cdot(b_d+l_{ap})\cdot(l_w+l_{ap})},\ R_{gp2}=\frac{l_{as}}{\mu_0\cdot(2b_d+l_{as})\cdot(l_w+l_{as})} \quad (13)$$

$$R_{gs2}=\frac{l_{as}}{\mu_0\cdot(2b_d+l_{as})\cdot(l_w+l_{as})},R_{gs1}=\frac{l_{as}}{\mu_0\cdot(b_d+l_{as})\cdot(l_w+l_{as})}$$

where μ_0 is the permeability of the air; μ_r and μ_s are the relative permeability of the core and the shunt, respectively. A_c is the effective cross-sectional area of the core. Other quantities can be found in Fig.6. Considering the fringing effect, the literature [36] points out an effective cross section of air gap with dimensions a by b would become $(a+g)$ by $(b+g)$. g is the length of the air gap. This consideration is included in the expression of R_{gp1}, R_{gp2}, R_{gs1}, R_{gs2}.

The expression for the leakage inductance calculation based on the equivalent reluctance models shown in Fig.7 is very bulky. But it can be simplified when the air gap length l_{ap} is identical to the l_{as},

$$l_{ap}=l_{as}=l_a \quad (14)$$

It leads to

$$R_{gp1}=R_{gs1}=R_{g1},\quad R_{gp2}=R_{gs2}=R_{g2} \quad (15)$$

Define R_m as

$$R_m=R_{c1}+R_{c2}+2R_{cc}+R_{s1}+2R_{ss} \quad (16)$$

The leakage inductance due to the magnetic shunt referred to the primary side is

$$L_{k\_shunt}=\frac{4k_p{}^2N_p{}^2}{R_m+R_{g1}+2R_{g2}+2R_{s2}} \quad (17)$$

Combining (7), (10), (11), (12) and (17), the total leakage inductance referred to the primary side for the above shunt-inserted transformer is

$$L_k=2\mu_0l_w\frac{n_p{}^2}{b_w}(\mathrm{x}_p+\mathrm{x}_s)+\frac{4n_p{}^2}{R_m+R_{g1}+2R_{g2}+2R_{s2}}$$
$$+\frac{1}{3}\mu_0\frac{l_w}{b_w}k_p{}^2\sum_{i=p,s}\left[2h_iN_i{}^3+h_{\Delta i}\left(2N_i{}^3-3N_i{}^2+N_i\right)\right] \quad (18)$$

where $n_p=k_p\cdot N_p$ is total number of turns for primary winding.

IV. Design Considerations

A. *Verification of the proposed calculation method*

TABLE I. Parameters of the Transformer

Parameters	Transformer *T1*
Turns per layer in primary k_p	2
Primary layers N_p	4
Primary conductor thickness h_p(mm)	0.07
Insulation thickness in primary $h_{\Delta p}$(mm)	0.2
Turns per layer in secondary k_s	1
Secondary layers N_s	2
Secondary conductor thickness h_s(mm)	0.07
Insulation thickness in secondary $h_{\Delta s}$(mm)	0.2

2-D Finite Element Analysis (FEA) simulations are carried out to verify the correctness of the equation (18). Details of

This article has been accepted for publication in a future issue of this journal, but has not been fully edited. Content may change prior to final publication. Citation information: DOI 10.1109/TPEL.2018.2842029, IEEE Transactions on Power Electronics

planar transformers parameters are given in TABLE I. The air gap length and the magnetic shunt thickness are kept constant, which are $2l_a$=0.2mm and t_{sh}=0.2mm. Fig.8 shows comparison between a the lumped calculation and the FEA simulation for the leakage inductance with different relative permeability of the shunt: 1) μ_s=10; 2) μ_s=30; 3) μ_s=60; 4) μ_s=120; 5) μ_s=200. The comparison between the proposed calculation method and the FEA simulation for the leakage inductance in the proposed configuration is shown in Fig.8. The calculation method for the shunt-inserted planar transformer represents good agreement with the FEA simulation.

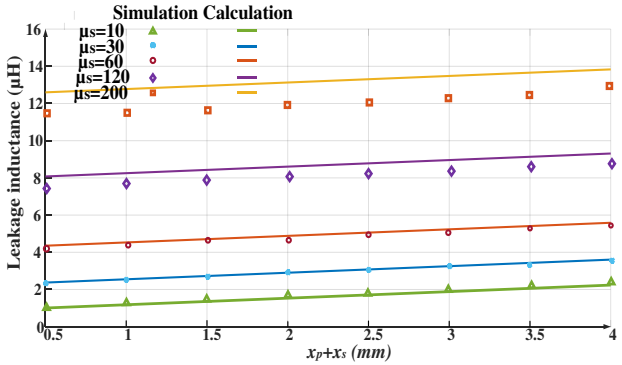

Fig.8. Comparison of leakage inductance obtained by FEA simulations and the proposed calculation method[31]

TABLE II. PARAMETERS OF THREE TESTS

Parameters	Three tests		
	Test 1	*Test 2*	*Test 3*
x_p(mm)	2	0	0
x_s(mm)	2	0	0
t_{sh} (mm)	0.15	0.15	0.3
$2l_a$ (mm)	0.1	0.1	0.1
μ_s	45	45	45

Three experiment tests were performed by using Agilent 4294A at 1MHz to further prove the calculation. The thickness and the relative permeability of the magnetic shunt, the distance from the primary winding and the secondary winding to the shunt, and the air gap length are documented in TABLE II while other parameters are kept same with TABLE I. Secondary windings were connected in a short circuit when measuring the leakage inductance referred to the primary side. The comparison between the calculation and the experiment tests is shown in Fig.9. Comparing the test 1 to the test 2, it is observed that the distance in between the primary and secondary windings to the shunt can create additional leakage inductance. Comparing the test 2 to the test 3, the leakage inductance is increased with the increased shunt thickness.

In high frequency (above 1MHz) LLC resonant converter design, typically the value of resonant inductance is not very large. Therefore the magnetic shunt with smaller relative permeability is more preferable. Moreover, both primary and secondary windings should be arranged away from the air gaps to minimize the fringing effect so as to achieve a smaller AC resistance.

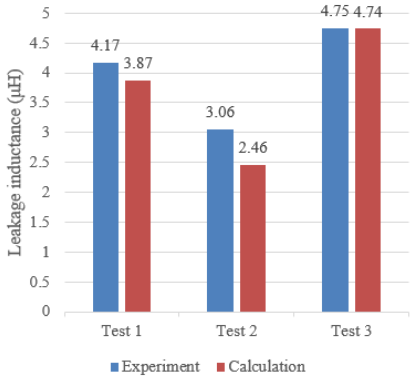

Fig.9. Experimental and calculation results comparison

B. Design guideline of the proposed transformer

It is predictable that the magnetizing inductance is also affected by the magnetic shunt, meaning that both leakage and magnetizing inductance are coupled. Moreover, the winding loss should also be investigated to achieve high efficiency.

In order to obtain desirable magnetizing and leakage inductance for LLC converter, the characteristics of the transformer are analyzed as follows. The expression for the magnetizing inductance is

$$L_m = \frac{2n_p{}^2 R_{s2}}{\left(R_m + R_{g1} + 2R_{g2}\right)\left(R_m + R_{g1} + 2R_{g2} + 2R_{s2}\right)} \tag{19}$$

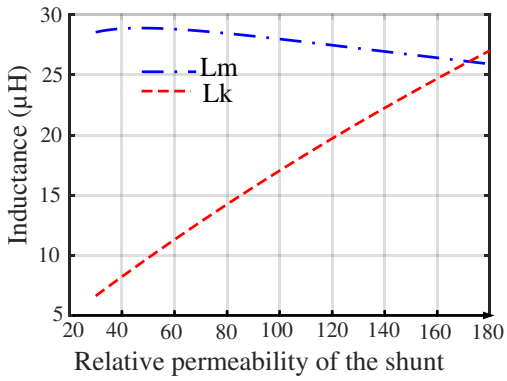

(a)

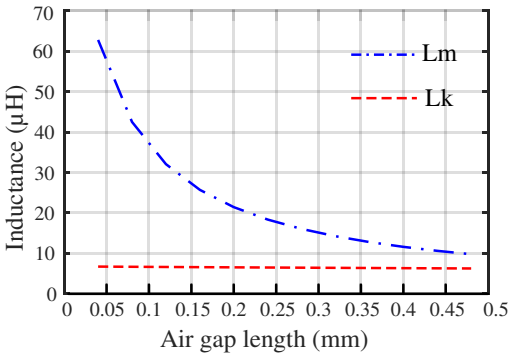

(b)

Fig.10. Comparison of L_m and L_k with constant x_p=x_s=2mm , t_{sh}=0.5mm (a)$2l_a$=0.14mm and varied μ_s (b) μ_s=30 and varied $2l_a$.

This article has been accepted for publication in a future issue of this journal, but has not been fully edited. Content may change prior to final publication. Citation information: DOI 10.1109/TPEL.2018.2842029, IEEE Transactions on Power Electronics

Once the magnetic core is chosen, only five parameters can affect magnetizing inductance and leakage inductance: the relative permeability of the magnetic shunt μ_s and its thickness t_{sh}, the air gap length l_a, the distances x_p and x_s. From the expression of (18) and (19), the distances x_p and x_s only influence the leakage inductance L_k. Fig.10 shows the influence of the relative permeability μ_s and air gap length l_a on magnetizing and leakage inductances. As illustrated in Fig.10(a), μ_s can influence the leakage inductance much more than the magnetizing inductance. On the contrary, the magnetizing inductance is mainly affected by the air gap length, which has a small effect on the leakage inductance as shown in Fig.10(b).

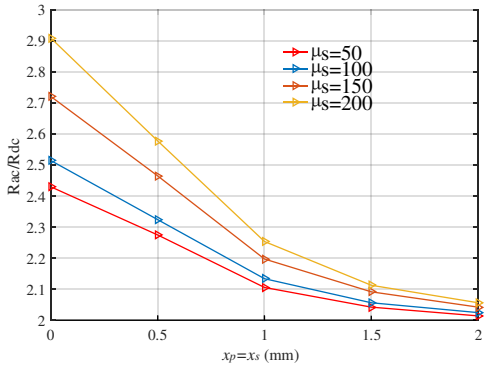

Fig.11. Investigation of AC resistance at 1MHz as a function of the distance from the shunt to windings for different μ_s

However, both primary and secondary windings must be placed away from the shunt to avoid fringing effect due to the air gap. This means that the distances x_p and x_s to separate windings and the shunt should be as far as possible. This is illustrated in Fig.11. 2D-FEA simulations were conducted to obtain the ratio of AC resistance to DC resistance at 1MHz. The transformer and winding details are the same with those in TABLE I. The relative permeability of the shunt varies from 50 to 200 and the shunt thickness is 0.2mm. It can be seen that the AC resistance is decreasing as the distances x_p and x_s increase, and a larger μ_s creates a larger AC resistance. Fortunately, the value of resonant inductance is not very large at high frequency LLC resonant converters. Thus the magnetic shunt with smaller relative permeability is more preferable.

C. High efficiency LLC resonant converter design considerations

TABLE III. CIRCUIT SPECIFICATIONS

Parameters	Values
Input voltage V_{in}	280-380V
Output voltage V_o	48V
Output power P_o	100W

The LLC converter specifications are shown in TABLE III. The key part of LLC resonant converter is the resonant tank, which includes the resonant capacitor C_r, resonant inductor L_r and the magnetizing inductance L_m. In this design, the resonant inductor L_r is integrated into the shunt-inserted planar transformer. The magnetizing inductance is always related to the primary and secondary RMS currents. In other words, it is well connected with the power loss of LLC converter. The optimal magnetizing inductance can be obtained from the analysis of power loss.

(a) Conduction and Switching Losses on Semi-conductors

Primary and secondary RMS currents are given in [34].

$$I_{RMS\_pri}=\frac{1}{4\sqrt{2}}\frac{V_o}{nR_L}\sqrt{\frac{n^4R_L^{\,2}T_s^{\,2}}{L_m^{\,2}}+4\pi^2+\frac{16\pi^2\left(T_st_d+t_d^{\,2}\right)}{T_s^{\,2}}} \tag{20}$$

$$I_{RMS\_sec}=\frac{\sqrt{3}}{24\pi}\frac{V_o}{R_L}\sqrt{\frac{\left(5\pi^2-48\right)n^4R_L^{\,2}T_s^{\,3}}{L_m^{\,2}\left(T_s+2t_d\right)}+\frac{12\pi^4T_s}{T_s+2t_d}+\frac{48\pi^4\left(T_st_d+t_d^{\,2}\right)}{T_s\left(T_s+2t_d\right)}} \tag{21}$$

where V_o is the output voltage; n is the transformer turns ratio; R_L is the load resistance; t_d is the dead time; T_s is the switching period at resonant frequency. From these two equations, the conduction losses for primary and secondary devices are described as follows:

$$P_{p\_c}=2I_{pri\_RMS}^{\,2}R_{p\_DS(\mathrm{on})} \tag{22}$$

$$P_{s\_c}=2I_{\mathrm{sec}\_RMS}^{\,2}R_{s\_DS(\mathrm{on})} \tag{23}$$

where $R_{p\_DS(on)}$ and $R_{s\_DS(on)}$ are the drain-to-source resistance of primary devices and secondary devices, respectively. Note that the expression (23) is only applicable when synchronous rectification is applied to secondary devices.

Since LLC converter can achieve ZVS turn-on, only turn-off loss P_{off} for the primary devices switching loss is taken into account [34]

$$P_{off}=\frac{V_{in}}{3}\left(\frac{V_o}{4nL_mf_r}-C_{pri\_oss}\frac{V_{in}}{T_{off}}\right)T_{off}f_r \tag{24}$$

where T_{off} is the turn-off time; C_{pri_oss} is the output capacitance of primary devices.

(b) Transformer losses

Planar transformer is suitable for high frequency converters due to its very low profile and excellent thermal characteristics [37]. Transformer losses consist of core loss and winding loss. The peak flux density is calculated following by the Faraday's law,

$$B_p=\frac{nV_o\left(T_s/2-T_d\right)}{2N_PA_e} \tag{25}$$

Considering hysteresis loss and eddy current loss, the core loss is calculated by $P_{core}=P_vV_e$, where V_e is the volume of the core and P_v is calculated by Steinmetz's equation: $P_v=K_cf^{\alpha}B_p^{\beta}$. These three quantities K_c, α and β can be calculated from relationship curve between unit volume core loss and flux density given in the datasheet of magnetic material. Thus the core loss can be obtained by

$$P_{core}=K_cf^{\alpha}\left(\frac{nV_o\left(T_s/2-T_d\right)}{2N_PA_e}\right)^{\beta}V_e \tag{26}$$

Dowell's model is the common method to calculate AC

This article has been accepted for publication in a future issue of this journal, but has not been fully edited. Content may change prior to final publication. Citation information: DOI 10.1109/TPEL.2018.2842029, IEEE Transactions on Power Electronics

winding loss, but its accuracy is affected by the fringing effect due to the air gap. The accurate winding loss can be estimated from 2-D FEA simulations [38]. The copper thickness is selected to be 2oz according to the skin effect at 1MHz.

(c) Magnetic shunt loss

The magnetic shunt loss limits the maximum power level. Losses within the magnetic shunt can be approximately estimated by a complex permeability μ''. The expression for the average rate of energy loss is [39]

$$P_{shunt\_av} = \frac{1}{2}\mu'' \omega h_o^2 \tag{27}$$

where ω is the angular frequency; h_o is the peak value of the applied magnetic field. The complex permeability μ'' of the magnetic shunt can be found from the datasheet. It can be seen that losses within magnetic shunt is dependent on the operating frequency, applied magnetic field and material complex permeability.

(d) Driving losses

As the converter operating at high frequency, the driving losses may not be neglected. It contains the losses for driving primary switches and secondary synchronous rectifiers,

$$P_{dr} = 2Q_{gs}V_{gs}f_s + 2Q_{gs\_sr}V_{gs\_sr}f_s \tag{28}$$

where V_{gs} and V_{gs_sr}, Q_{gs} and Q_{gs_sr} represent the driving voltages and the gate-source charge for the primary and secondary devices, respectively.

Therefore, the total power loss of the half bridge LLC resonant converter is

$$P_{total} = P_{p\_c} + P_{s\_c} + P_{off} + P_{core} + P_{winding} + P_{dr} + P_{shunt\_av} \tag{29}$$

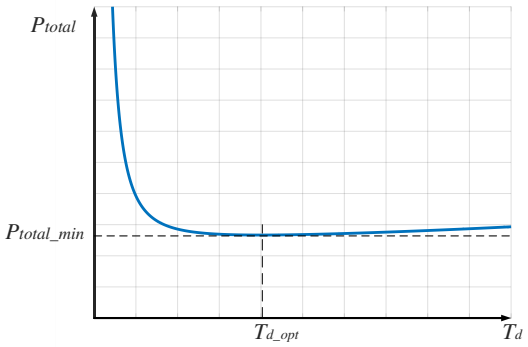

Fig.12. Total power loss as a function of dead time[31]

It can be concluded that the magnetizing inductance should be maximized as possible to reduce power loss. Meanwhile, as the magnetizing current should discharge all parasitic capacitances during the dead time, it needs to be smaller enough to allow sufficient magnetizing current to discharge all parasitic capacitances. Thus the magnetizing inductance should be designed to be the largest value that guarantees ZVS. According to [35],

$$L_m = \frac{t_d\left((T_s/2) - t_d\right)}{4\left(2C_{pri\_oss} + 2C_{sec\_oss}/n^2 + C_w\right)} \tag{30}$$

where C_{sec_oss} is the secondary device charge equivalent output capacitance, C_w is the transformer winding capacitance referred to the primary side. The equation (30) gives an optimal magnetizing inductance expressed by the dead time. To determine the optimal magnetizing inductance, the total power loss as a function of the dead time, is shown in Fig.12. The optimal T_d can be selected in according with the minimum loss point and then L_m can be determined by the equation (30) with the selected dead time.

V. Experimental Implementation

TABLE IV. Circuit Parameters

Parameters	Values
Magnetizing inductance L_m	26μH
Resonant inductance L_r	3.5μH
Resonant capacitance C_r	7.23nF
Turns-ratio n	8:2:2
Primary devices	GS66504B
Secondary devices	BSZ240N12NS3
Core type and material	E32/6/20-3F46

TABLE V. Parameters Of The Designed Transformer

Parameters	Transformer
Turns per layer in primary k_p	2
Primary layers N_p	4
Primary conductor thickness h_p(mm)	0.07
Insulation thickness in primary $h_{\Delta p}$(mm)	0.25
Turns per layer in secondary k_s	1
Secondary layers N_s	4
Secondary conductor thickness h_s(mm)	0.07
Insulation thickness in secondary $h_{\Delta s}$(mm)	0.25
Magnetic shunt material	IFL04
Shunt thickness t_{sh}(mm)	0.1
Air gap length $2l_a$(mm)	0.18
Permeability of magnetic shunt μ_s	45
Distance between primary windings and the shunt x_p (mm)	2
Distance between primary windings and the shunt x_s (mm)	2

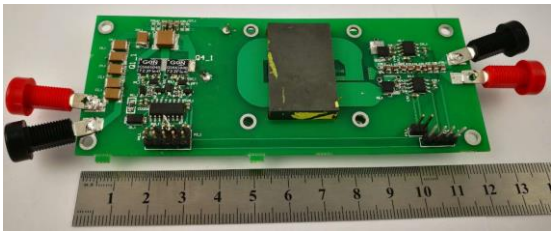

Fig.13. Prototype of 1MHz 100W LLC resonant converter

A 1 MHz, 100W half bridge LLC resonant converter is built, as shown in Fig.13. Detailed circuit parameters and the

This article has been accepted for publication in a future issue of this journal, but has not been fully edited. Content may change prior to final publication. Citation information: DOI 10.1109/TPEL.2018.2842029, IEEE Transactions on Power Electronics

proposed planar transformer parameters are listed in TABLE IV and TABLE V, respectively. In this design, the resonant inductor is integrated into the planar transformer by using its leakage inductance created by the magnetic shunt. The material for the magnetic shunt used here is IFL04. The selected inductance ratio is 7.4 to narrow the switching frequency band. The magnetic core used in the transformer is E32/6/20-3F46 and the 8:2:2 turns ratio is used to achieve optimal magnetizing and leakage inductance. GS66504B from GaN system is selected for the primary devices due to its low effective output capacitance and on-state resistance compared with the silicon devices.

Waveforms of the converter operating at resonant frequency (1 MHz) with 380V input and 48V output is shown in Fig.14(a). To guarantee GaN devices in a safe operation, the output gate signal from gate driver has negative turn-off voltage. It can be seen that the ZVS turn-on is achieved because the drain-to-source voltage drops to zero and then the gate turns on immediately. Thus the reverse conduction through GaN devices is greatly minimized. Fig.14(b) shows the waveforms of the converter operating at 700 kHz with 280V input and 48V-100W output, and the ZVS operation is also achieved.

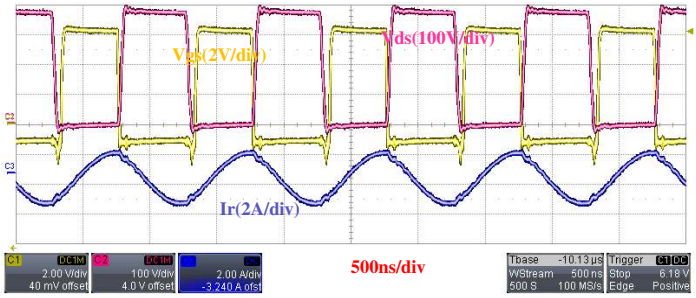

(a)

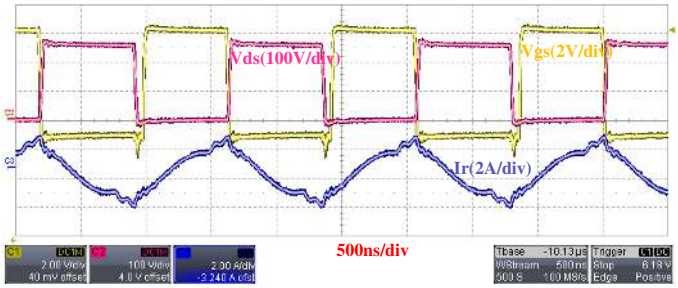

(b)

Fig.14. 100W LLC resonant converter with shunt integrated transformer operating at (a) 1MHz with 380V input (b) 700kHz with 280V input

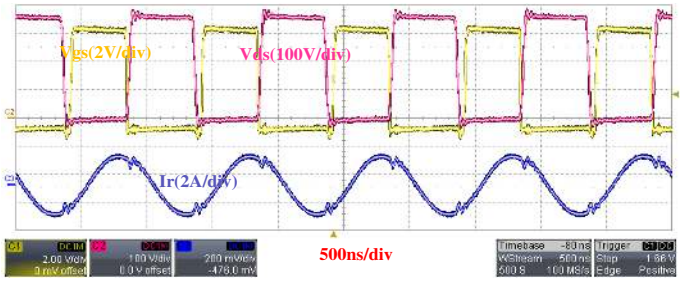

(a)

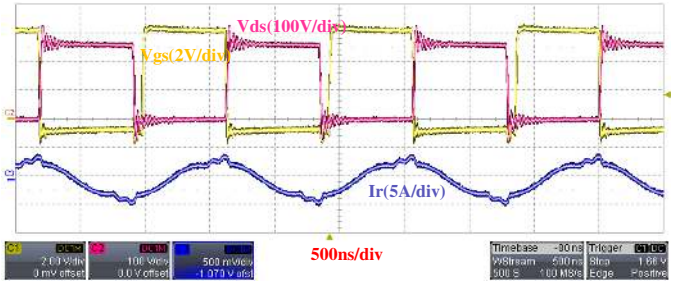

(b)

Fig.15. 100W LLC resonant converter with discrete magnetics operating at (a) 1MHz with 380V input (b) 700kHz with 280V input

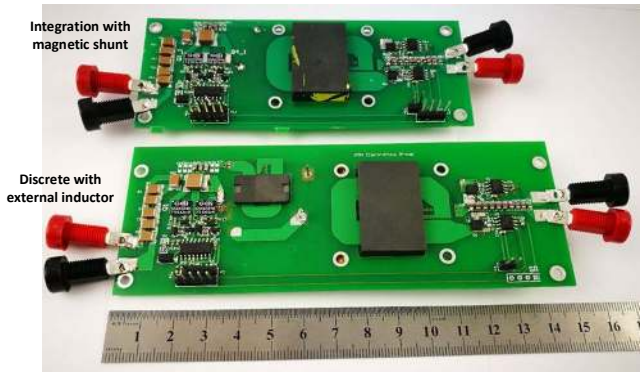

Fig.16. Size comparison of two converters: upper is with magnetic shunt and lower is with external inductor

Due to the small inductance ratio, switching frequency range is greatly narrowed. Switching frequency swings from 700 kHz to 1MHz to accommodate input voltage changing from 280V to 380V. To prove the LLC converter with integrated magnetic shunt transformer can achieve comparable performance with the one discrete magnetic component, the converter using planar transformer with external inductor is built for the comparison. To conduct a fair comparison, the discrete version has the same parameters and components with the converter with integrated magnetic shunt. The external inductor is made by PCB planar inductor with EI 18/4/10 core shape with 0.18mm air gaps situated in each leg and 3F46 Ferrite material, and 3 turns with one turn each layer. The resonant inductance is the sum of the transformer leakage inductance and external inductance created by the PCB planar inductor. Some waveforms are captured and shown in Fig.15. Fig. 16 shows the photos of the two prototypes and the integrated converter has nearly 20% size reduction compared to the discrete converter.

Efficiency curves of the two converters under different input voltages and load conditions are illustrated in Fig.17. The peak efficiency of the LLC converter with magnetic shunt integrated transformer at resonant frequency is around 95%. When input voltage decreases to 280V, the switching frequency decreases to 700 kHz to achieve the corresponding voltage gain and the efficiency in this case drops around 1.5% at full power. It can also be observed that both cases can achieve almost the same efficiency under the entire load conditions. This verifies the optimal design guideline for the proposed transformer. It can not only regulate a wider voltage range with the low inductance ratio due to the large leakage inductance created by the

This article has been accepted for publication in a future issue of this journal, but has not been fully edited. Content may change prior to final publication. Citation information: DOI 10.1109/TPEL.2018.2842029, IEEE Transactions on Power Electronics

magnetic shunt, but also increase power density of the whole converter because of this magnetic integration method. Thus the proposed transformer is well adapted to LLC resonant converter.

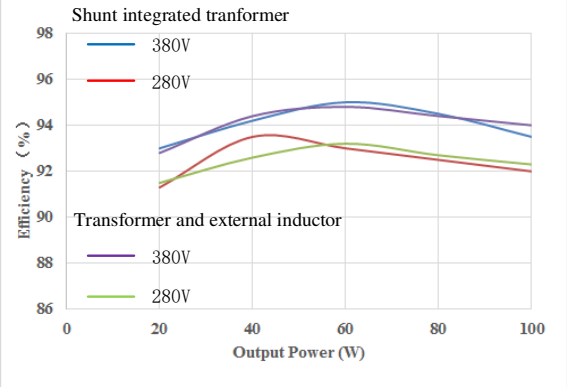

Fig.17. Efficiency of LLC converter at different load conditions

The loss breakdown of the converter with shunt integrated transformer at 1MHz with 380V input and 48V-100W output is shown in Fig.18. The transformer loss is dominating, which is about 45% of the total loss. The GaN devices and secondary MOSFETs take 38% of the total loss. Loss from the magnetic shunt is around 0.8W and accounts for 17% of total loss.

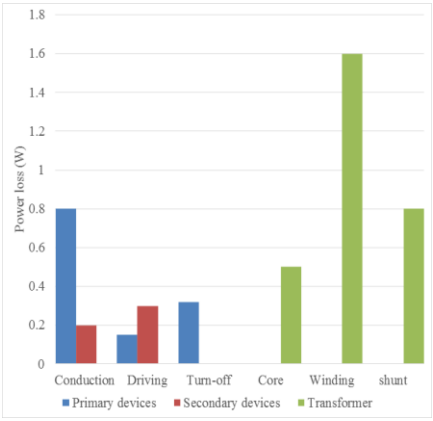

Fig.18. Loss breakdown for the converter with shunt integrated transformer operating at 1MHz with 380V input and 48V-100W output

VI. Conclusion

In this paper, a planar transformer structure with a magnetic shunt is proposed to create a large leakage inductance. The leakage inductance calculation methodology is verified by 2-D FEA simulations and experiment tests. Detailed design considerations for the proposed transformer and high performance LLC resonant converter are given. The prototype proves that the transformer structure is well adapted to integrate a larger resonant inductor into the transformer of LLC resonant converter. Moreover, the proposed transformer structure and design methodology maintain an optimal magnetizing inductance while increasing leakage inductance to obtain a narrowed switching frequency band, so that high efficiency is achieved under wide input voltage range. Experiment results show the converter with the proposed integrated transformer obtains the same regulation capability and comparable efficiency with the converter using discrete magnetic components. This verifies the optimal design guideline for the proposed transformer. Moreover, the power density is increased due to this magnetic integration method. Thus the proposed transformer is well adapted to LLC resonant converter. The application of magnetic shunt can be further extended to other topologies since it can integrate the series inductor connected with transformer, for example, phase-shifted full bridge converters (PSFB), and dual active bridge converters (DBA).

References

[1] Czarkowski, D., and M.k. Kazimierczuk. “Phase-Controlled CLL Resonant Converter.” Proceedings Eighth Annual Applied Power Electronics Conference and Exposition,1993, pp. 432–438, 1993.

[2] M. Kazimierczuk and X. Bui, “Class E DC/DC converters with an inductive impedance inverter,” IEEE Transactions on Power Electronics, vol. 4, no. 1, pp. 124–135, 1989.

[3] M. Kazimierczuk, M. Mescher, and R. Prenger, “Class D current-driven transformer center-tapped controllable synchronous rectifier,” IEEE Transactions on Circuits and Systems I: Fundamental Theory and Applications, vol. 43, no. 8, pp. 670–680, 1996.

[4] C. Fei, F. C. Lee, and Q. Li, “High-efficiency High-power-density LLC Cocnverter with an Integrated Planar Matrix Transformer for High Output Current Applications,” IEEE Transactions on Industrial Electronics, pp. 1–1, 2017.

[5] B. Yang and F. C. Lee, “LLC Resonant Converter for Front End DC / DC Conversion,” Applied Power Electronics Conference and Exposition, vol. 2,pp. 1108–1112, 2002

[6] Z. Fang, T. Cai, S. Duan, and C. Chen, “Optimal Design Methodology for LLCResonant Converter in Battery Charging Applications Based on Time-Weighted Average Efficiency,” IEEE Transactions on Power Electronics, vol. 30, no. 10, pp. 5469–5483, 2015.

[7] M. Noah, S. Kimura, S. Endo, M. Yamamoto, J. Imaoka, K. Umetani, and W. Martinez, “A novel three-phase LLC resonant converter with integrated magnetics for lower turn-off losses and higher power density,” 2017 IEEE Applied Power Electronics Conference and Exposition (APEC), 2017.

[8] W. Sun, Y. Xing, H. Wu, and J. Ding, “Modified High-efficiency LLC Converters with Two Split Resonant Branches for Wide Input-Voltage Range Applications,” IEEE Transactions on Power Electronics, pp. 1–1, 2017.

[9] X. Mathu, C. O. Na, W. Ningning, S. Kulkarni, and S. Roy, “Review of integrated magnetics for power supply on chip (PwrSoC),” IEEE Trans. Power Electron., vol. 27, no. 11, pp. 4799–4816, Nov. 2012.

[10] K. Bong-Chul, P. Ki-Bum, K. Chong-Eun, L. Byoung-Hee, and M. Gun-Woo, “LLC resonant converter with adaptive link-voltage variation for a high-power-density adapter,” IEEE Trans. Power Electron., vol. 25, no. 9, pp. 2248–2252, Sep. 2010.

[11] A. Kwasinski and C. N. Onwuchekwa, “Dynamic behavior and stabilization of DC microgrids with instantaneous constant-power loads,” IEEE Trans. Power Electron., vol. 26, no. 3, pp. 822–834, Mar. 2011.

[12] Y. Jeong, G.-W. Moon, and J.-K. Kim, “Analysis on half-bridge LLC resonant converter by using variable inductance for high efficiency and power density server power supply,” 2017 IEEE Applied Power Electronics Conference and Exposition (APEC), 2017.

[13] Y. Chen, H. Wang, Z. Hu, Y.-F. Liu, J. Afsharian, and Z. A. Yang, “LCLC resonant converter for hold up mode operation,” 2015 IEEE Energy Conversion Congress and Exposition (ECCE), 2015.

[14] Kim, Dong-Kwan, et al. "High-efficiency LLC resonant converter with high voltage gain using an auxiliary LC resonant

circuit." IEEE Transactions on Power Electronics,vol. 31, no. 10, pp. 6901-6909, 2016.
[15] Chul Wan Park, Sang Kyoo Han "Design of an integrated magentics structure for LLC resonant converter." IECON 2017-43h Annual Conference of the IEEE Industrial Electronics Society, 2017
[16] Yang, Bo, Rengang Chen, and Fred C. Lee "Integrated magentics for LLC resonant converter." Applied Power Electronics Conference and Exposition, 2002. APEC 2002. Seventeenth Annual IEEE. Vol. 1. IEEE, 2002.
[17] Cezary Worek, Sławomir Ligenza " Integrated magnetic element for improving efficiency of LLC resonant converter." 2017 IEEE Energy Conversion Congress and Exposition (ECCE), 2017
[18] Jee-Hoon Jung, "Bifilar Winding of a Center-Tapped Transformer Including Integrated Resonant Inductance for LLC Resonant Converters," in IEEE Transactions on Power Electronics, vol. 28, no. 2, pp. 615-620, 2013.
[19] B.-C. Kim, K.-B. Park, C.-E. Kim, B.-H. Lee, and G.-W. Moon, "LLC resonant converter with adaptive link-voltage variation for a high-powerdensity adapter," IEEE Trans. Power Electron., vol. 25, no. 9, pp. 2248– 2252, Sep. 2010.
[20] J.-Y. Lee, Y.-S. Jeong, and B.-M. Han, "An isolated dc/dc converter using high-frequency unregulated LLC resonant converter for fuel cell applications," IEEE Trans. Ind. Electron., vol. 58, no. 7, pp. 2926–2934, Jul. 2011
[21] D. Huang, S. Ji and F. C. Lee, "LLC Resonant Converter With Matrix Transformer," in IEEE Transactions on Power Electronics, vol. 29, no. 8, pp. 4339-4347, Aug. 2014.
[22] B. Li, Q. Li, and F. C. Lee, "A novel PCB winding transformer with controllable leakage integration for a 6.6kW 500kHz high efficiency high density bi-directional on-board charger," in 2017 IEEE Applied Power Electronics Conference and Exposition (APEC), pp. 2917–2924, 2017.
[23] D. Fu, F. C. Lee and Shuo Wang, "Investigation on Transformer Design of High Frequency High Efficiency DC-DC Converters," in Proc. of IEEE APEC, pp. 940-947, 2010.
[24] Q. Wang, X. Zhang, R. Burgos, D. Boroyevich, A. White, and M. Kheraluwala, "Design considerations for a high efficiency 3 kW LLC resonant DC/DC transformer," in Energy Conversion Congress and Exposition (ECCE), 2015 IEEE, pp. 5454-5461, 2015.
[25] K. Tan, R. Yu, S. Guo, and A. Q. Huang, "Optimal design methodology of bidirectional LLC resonant DC/DC converter for solid state transformer application," IECON 2014 - 40th Annual Conference of the IEEE Industrial Electronics Society, 2014.
[26] Zhang, Y., Xu, D., Mino, K., and Sasagawa, K. "1 MHz–1 kW LLC resonant converter with integrated magnetics". IEEE Applied Power Electronics Conf. Exposition (APEC) 2007, Anaheim, CA, USA, February 2007, pp. 955–961
[27] Microelectronics S T. "LLC resonant converter half-bridge converter design guideline". Application note, 2007
[28] Yang, B., Chen, R., and Lee, F.C. "Integrated magnetics for LLC resonant converter". IEEE Applied Power Electronics Conf. Exposition (APEC) 2002, Dallas, TX, USA, March 2002, pp. 346–351
[29] J. Zhang, Z. Ouyang, M. C. Duffy, M. A. E. Andersen, and W. G. Hurley, "Leakage inductance calculation for planar transformers with a magnetic shunt," IEEE Transactions on Power Electronics, vol. 50, no. 6, pp.4107-4112. 2014.
[30] M.-X. Li, Z. Ouyang, B. Zhao, M.A. E. Andersen，"Analysis and Modeling of Integrated Magnetics for LLC resonant Converters" IECON 2017- 43h Annual Conference of the IEEE Industrial Electronics Society, Beijing, 2017, pp. 834-839.
[31] M.-X. Li, Z. Ouyang, B. Zhao, M.A. E. Andersen， "High Frequency LLC Resonant Converter with Magnetic Shunt Integrated Planar Transformer" 2018 IEEE Applied Power Electronics Conference and Exposition (APEC), 2018.
[32] Z. Ouyang, J. Zhang, and W. G. Hurley, "Calculation of Leakage Inductance for High-Frequency Transformers," IEEE Transactions on Power Electronics, vol. 30, no. 10, pp. 5769–5775, 2015.
[33] Z. Ouyang, O. C. Thomsen, and M. A. E. Andersen, "Optimal design and tradeoff analysis of planar transformer in high-power dc–dc converters," IEEE Trans. Ind. Electron., vol. 59, no. 7, pp. 2800–2810, Jul. 2012.
[34] J.-Y. Lee, Y.-S. Jeong, and B.-M. Han, "An Isolated DC/DC Converter Using High-Frequency Unregulated LLC Resonant Converter for Fuel Cell Applications," IEEE Transactions on Industrial Electronics, vol. 58, no. 7, pp. 2926–2934, 2011.
[35] W. Zhang, F. Wang, D. J. Costinett, L. M. Tolbert and B. J. Blalock,"Investigation of Gallium Nitride Devices in High-Frequency LLC Resonant Converters," IEEE Transactions on Power Electronics, vol.32, no. 1, pp. 571-583, Jan. 2017.
[36] W. G. Hurley and W. H. Wölfle, "Transformers and Inductors for Power Electronics," Aug. 2013.
[37] Z. Ouyang and Michael A. E. Andersen. "Overview of Planar Magnetic Technology—Fundamental Properties." IEEE Transactions on Power Electronics, vol. 29, no. 9, 2014, pp. 4888–4900.
[38] B. Li, Q. Li, and F. C. Lee, "A novel PCB winding transformer with controllable leakage integration for a 6.6kW 500kHz high efficiency high density bi-directional on-board charger," IEEE Applied Power Electronics Conference and Exposition (APEC), 2017.
[39] Coey J. M. D. "Magnetism and magnetic materials", Cambridge University Press, pp.440-466, 2010.

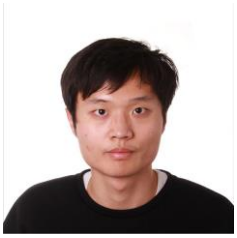

Mingxiao Li was born in Shandong, China, in 1995. He received the B.S degree in electrical engineering from Chongqing University, Chongqing, China, in 2016. He is currently a master student working toward power electronics from the Department of Electrical Engineering, Technical University of Denmark, Kongens Lyngby, Denmark.
His research interests include magnetics design, modeling and integration in power supplies, resonant converters and high frequency power conversion.

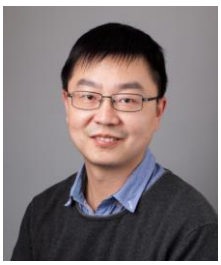

Ziwei Ouyang (S'07, M'11, SM'17) received his PhD degree from Technical University of Denmark (DTU) in 2011. From 2011 to 2013, he was a postdoc researcher at DTU. From 2013 to 2016, he was appointed as an assistant professor at the same department. Since from April 2016, he is an associate professor at DTU. His research areas focus on high-frequency planar magnetics modeling and integration, high-density high-efficiency power converters, PV battery energy storage system, and wireless charging etc.
He is IEEE senior member. He has over 60 high impact IEEE journal and conference publications, co-author on a book chapter on Magnetics for the "Handbook of Power Electronics" and currently he

is the holder of 8 international patents. He was a recipient of Young Engineer Award at PCIM-Asia 2014, and received Best Ph.D. Dissertation of the Year Award 2012 in Technical University of Denmark. He received several Best Paper Awards in IEEE sponsored international conferences. He has been invited to give lectures in many universities, enterprises and educational seminars and workshops around the world including USA, Europe and China. He has served as session chair in some IEEE sponsored conferences and reviewer for the IEEE Transactions on power electronics and IEEE Transactions on Industrial Electronics. Currently, he is responsible for the Power Electronics course for both undergraduate and graduate students at DTU, and he also supervised more than 40 students' projects including Postdoc, Ph.D. and Master projects.

Michael A.E. Andersen (M'88) received the M.Sc.E.E. and Ph.D. degrees in power electronics from the Technical University of Denmark, Kgs. Lyngby, Denmark, in 1987 and 1990, respectively. He is currently a Professor of power electronics at the Technical University of Denmark, where since 2009, he has been the Deputy Head of the Department of Electrical Engineering. He is the author or coauthor of more than 300 publications. His research interests include switch-mode power supplies, piezoelectric transformers, power factor correction, and switch-mode audio power amplifiers.